materials

Article

Synthesis, Molecular Structure and Cytotoxicity of Molecular Materials Based on Water Soluble Half-Sandwich Rh(III) and Ir(III) Tetranuclear Metalla-Cycles

Gajendra Gupta [1], **Benjamin S. Murray** [2], **Paul J. Dyson** [2] **and Bruno Therrien** [1,*]

[1] Institute of Chemistry, University of Neuchatel, Avenue de Bellevaux 51, Neuchatel CH-2000, Switzerland; E-Mail: gajendra.gupta@unine.ch

[2] Institute of Chemical Sciences and Engineering, Ecole Polytechnique Fédérale de Lausanne (EPFL), Lausanne CH-1015, Switzerland; E-Mails: benjamin.murray@epfl.ch (B.S.M.); paul.dyson@epfl.ch (P.J.D.)

* Author to whom correspondence should be addressed; E-Mail: bruno.therrien@unine.ch; Tel.: +41-32-718-2499; Fax: +41-32-718-2511.

Abstract: The neutral dinuclear complexes $[(\eta^5\text{-}C_5Me_5)_2Rh_2(\mu\text{-dhnq})Cl_2]$ (**1**) and $[(\eta^5\text{-}C_5Me_5)_2Ir_2(\mu\text{-dhnq})Cl_2]$ (**2**) (dhnqH$_2$ = 5,8-dihydroxy-1,4-naphthoquinone) were obtained from the reaction of $[(\eta^5\text{-}C_5Me_5)M(\mu\text{-Cl})Cl]_2$ (M = Rh, Ir) with dhnqH$_2$ in the presence of CH_3COONa. Treatment of **1** or **2** in methanol with linear ditopic ligands L (L = pyrazine, 4,4′-bipyridine or 1,2-bis(4-pyridyl)ethylene), in the presence of $AgCF_3SO_3$, affords the corresponding tetranuclear metalla-rectangles $[(\eta^5\text{-}C_5Me_5)_4M_4(\mu\text{-dhnq})_2(\mu\text{-L})_2]^{4+}$ (L = pyrazine, M = Rh, **3**; M = Ir, **4**; L = 4,4′-bipyridine, M = Rh, **5**; M = Ir, **6**; L = 1,2-bis(4-pyridyl)ethylene, M = Rh, **7**; M = Ir, **8**). All complexes were isolated as their triflate salts and were fully characterized by infrared, ^{1}H and ^{13}C NMR spectroscopy, and some representative complexes by single-crystal X-ray structure analysis. The X-ray structures of **3**, **5** and **6** confirm the formation of the tetranuclear metalla-cycles, and suggest that complexes **5** and **6** possess a cavity of sufficient size to encapsulate small guest molecules. In addition, the antiproliferative activity of the metalla-cycles **3–8** was evaluated against the human ovarian A2780 (cisplatin sensitive) and A2780cisR (cisplatin resistant) cancer cell lines and on non-tumorigenic human embryonic kidney HEK293 cells. All cationic tetranuclear metalla-rectangles were found to be highly cytotoxic, with IC$_{50}$ values in the low micromolar range.

1. Introduction

The biological application of coordination-driven arene ruthenium metalla-materials is a flourishing area of research [1–6]. The tetranuclear assemblies have been found to possess good anticancer activity [7–12], to strongly interact with DNA [13,14], and to efficiently detect biologically relevant analytes [15–17]. Their DNA binding can occur through non-covalent interactions, novel modes of action also observed for di- and trinuclear organometallics [18–20], although fragmentation inside cells followed by coordination of the metal ion to DNA and/or other biomolecules cannot be excluded. Following the promising studies of arene ruthenium metalla-materials, a series of cationic arene osmium metalla-rectangles were recently reported [21]. These arene osmium derivatives display comparable cytotoxicity to the ruthenium-based analogues, suggesting that the biological applications of arene ruthenium metalla-rectangles can be extended to other transition metals.

It is well known that the chemistry of arene ruthenium and arene osmium complexes is similar to that of half-sandwich rhodium and iridium complexes [22–25] and that several organometallic compounds of these metals with promising anticancer activity have been reported [26–29]. Moreover, several pentamethylcyclopentadienyl rhodium and iridium metalla-rectangles have been synthesized and structurally characterized by the group of Jin [30–32]. These metalla-rectangles show comparable structural and physico-chemical properties to the arene ruthenium analogues. However, the biological activity of these tetranuclear assemblies has not yet been explored. Therefore, to evaluate the anticancer properties of pentamethylcyclopentadienyl rhodium and iridium metalla-rectangles, a series of cationic tetranuclear complexes incorporating 5,8-dioxido-1,4-naphthoquinonato (dhnq) bridges and ditopic N-ligands [pyrazine, 4,4′-bipyridine and 1,2-bis(4-pyridyl)ethylene] has been prepared and their antiproliferative activity evaluated *in vitro* on human ovarian cancer cell lines (A2780 and A2780cisR) and on non-tumorigenic cells (HEK293). The anticancer activity of these pentamethylcyclopentadienyl rhodium and iridium metalla-rectangles was compared to that of $[(\eta^6\text{-}p\text{-Pr}^i\text{C}_6\text{H}_4\text{Me})_4\text{Ru}_4(\mu\text{-dhnq})_2(\mu\text{-}4,4'\text{-bipyridine})_2](\text{CF}_3\text{SO}_3)_4$ (Figure 1) [9].

Figure 1. Molecular structure of $[(\eta^6\text{-}p\text{-Pr}^i\text{C}_6\text{H}_4\text{Me})_4\text{Ru}_4(\mu\text{-dhnq})_2(\mu\text{-}4,4'\text{-bipyridine})_2](\text{CF}_3\text{SO}_3)_4$.
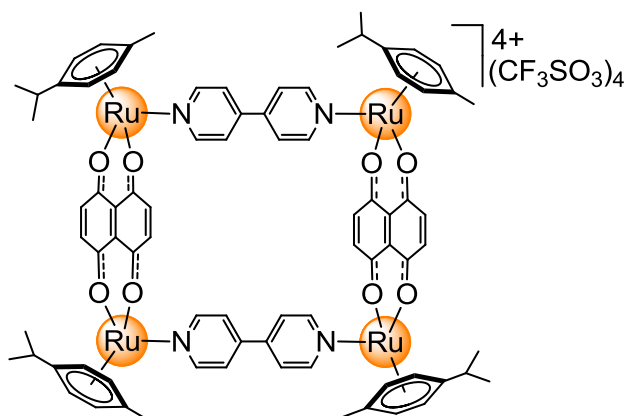
2. Results and Discussion

The reaction of the dinuclear pentamethylcyclopentadienyl complexes $[(\eta^5\text{-}C_5Me_5)M(\mu\text{-}Cl)Cl]_2$ (M = Rh and Ir) with dhnqH$_2$ (dhnqH$_2$ = 5,8-dihydroxy-1,4-naphthoquinone) in methanol in the presence of CH$_3$COONa leads to the formation of the neutral complexes $[(\eta^5\text{-}C_5Me_5)_2Rh_2(\mu\text{-dhnq})Cl_2]$ (**1**) and $[(\eta^5\text{-}C_5Me_5)_2Ir_2(\mu\text{-dhnq})Cl_2]$ (**2**). Addition of AgCF$_3$SO$_3$ to **1** and **2**, followed by addition of linear ditopic ligands L [L = pyrazine, 4,4′-bipyridine or 1,2-bis(4-pyridyl)ethylene], affords the cationic tetranuclear metalla-rectangles of the general formula $[(\eta^5\text{-}C_5Me_5)_4M_4(\mu\text{-dhnq})_2(\mu\text{-}L)_2]^{4+}$ (L = pyrazine, M = Rh, **3**; M = Ir, **4**; L = 4,4′-bipyridine, M = Rh, **5**; M = Ir, **6**; L = 1,2-bis(4-pyridyl)ethylene, M = Rh, **7**; M = Ir, **8**), see Scheme 1. The rectangular cations **3–8** are isolated as triflate salts. All complexes are non-hygroscopic and stable in air and have been fully characterized by analytical and spectroscopic techniques. The compounds are soluble in polar solvents and are insoluble in non-polar solvents. In addition, all the metalla-rectangles are soluble and stable in water and DMSO (dimethyl sulfoxide). Interestingly, the metalla-rectangles are stable for weeks in water, while in DMSO, new species only start to appear after 3–4 h in solution [determined by nuclear magnetic resonance (NMR)].

Scheme 1. Synthesis of tetranuclear metalla-rectangles **3–8** from **1** and **2**.
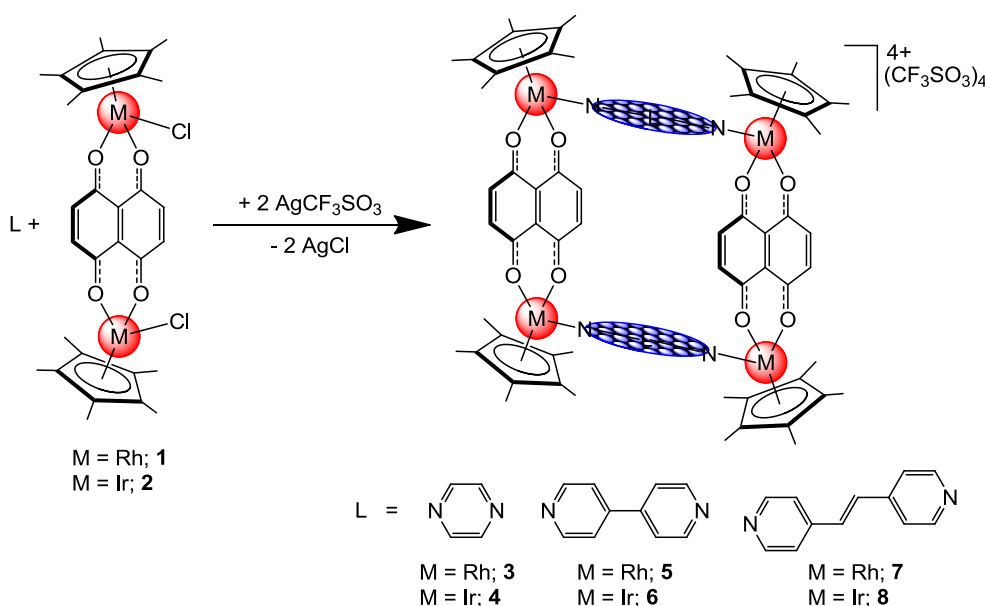
The ^{1}H NMR spectra of the complexes were recorded in CD$_2$Cl$_2$ at 25 °C and the chemical shifts of the different protons are listed in the experimental section. The ^{1}H NMR spectra of **1–8** contain a singlet resonance between 7.0 and 7.4 ppm that can be attributed to the protons of the dhnq bridges. Upon formation of the metalla-rectangles, the signals associated to the dhnq protons are shifted downfield relative to those of the neutral dinuclear complexes **1** (δ = 7.01 ppm) and **2** (δ = 7.09 ppm), see Figure 2. Similarly, the singlet of the pyrazine ligands is shifted downfield after formation of metalla-rectangles **3** and **4**. In contrast, the proton signals derived from the 4,4′-bipyridine and 1,2-bis(4-pyridyl)ethylene derivatives show a different trend after coordination, the H$_\alpha$ of the pyridyl groups are shifted upfield whereas the H$_\beta$ protons are shifted downfield, see Figure 2. The observed chemical shifts are consistent with the formation of the expected metalla-rectangles.

Figure 2. ^{1}H NMR spectra (aromatic region) of free pyrazine, 4,4′-bipyridine and 1,2-bis(4-pyridyl)ethylene, as well as the dinuclear complexes **1**–**2** and the metalla-rectangles **3**–**8** in CD_2Cl_2 (25 °C).
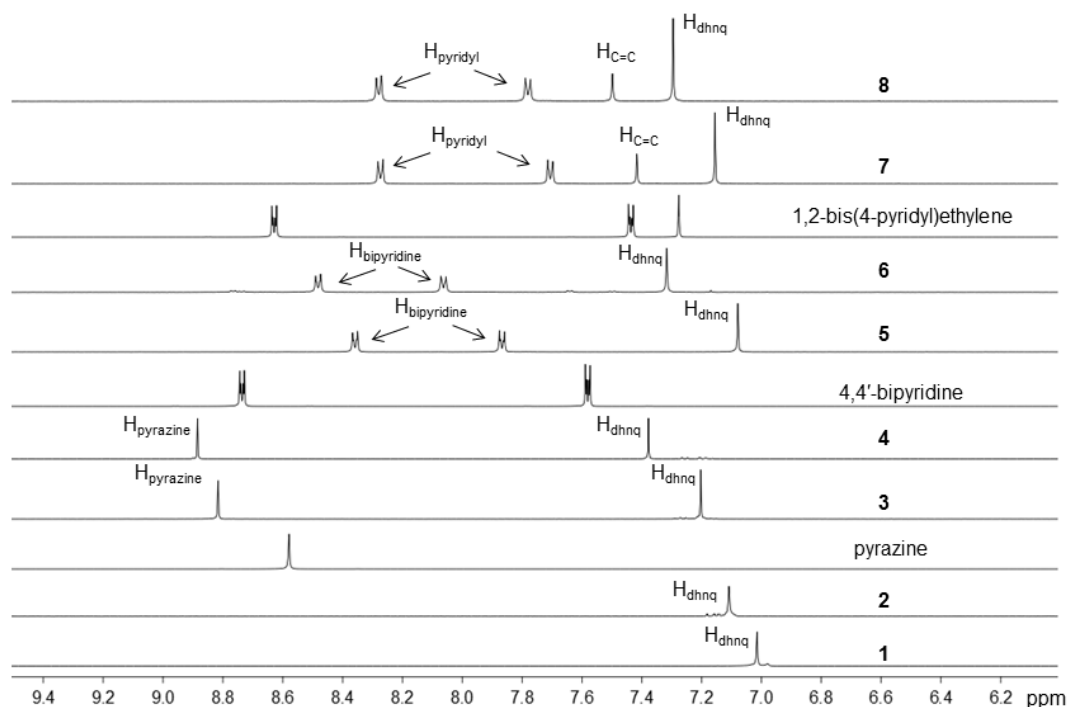
2.1. Molecular structures of 3, 5 and 6

Dark green crystals of the metalla-rectangles [**3**](CF_3SO_3)$_4$, [**5**](CF_3SO_3)$_4$ and [**6**](CF_3SO_3)$_4$, suitable for single-crystal X-ray structure analysis were obtained by addition of toluene to a dichloromethane solution of the respective complexes. All metalla-rectangles crystallize with solvent molecules and four triflate anions. The molecular structures of **3**, **5** and **6** are presented in Figures 3–5, respectively. Selected bond lengths and angles are listed in Table 1 and the crystallographic details are given in Table 2.

As expected, metalla-rectangle **3** is composed of two dinuclear [(η^5-C$_5$Me$_5$)$_2$Rh$_2$(μ-dhnq)]$^{2+}$ clips connected by two pyrazine ligands (Figure 3). The Rh-Rh distances are 6.9773(5) Å through the pyrazine units and 8.3831(5) Å through the dhnq bridges. In metalla-rectangles **5** and **6**, the dinuclear [(η^5-C$_5$Me$_5$)$_2$M$_2$(μ-dhnq)]$^{2+}$ clips are connected with 4,4′-bipyridine units, thus providing a much longer rectangle with metal-metal distances through the 4,4′-bipyridine ligands of 11.106(1) and 11.2437(7) Å for **5** and **6**, respectively. The metal-metal distances observed in these metalla-rectangles are comparable to those found in analogous half-sandwich metalla-assemblies incorporating either pyrazine, 4,4′-bipyridine or dhnq building blocks [33–35].

The cavity size of metalla-rectangles **5** and **6** is approximately 8 × 11 Å^2, while for metalla-rectangle **3** the cavity is 8 × 7 Å^2 (Table 1). Therefore, considering the size of the hydrophobic cavity and the presence of aromatic rings in the multiple components of the metalla-rectangles, the hydrophobic cavities of the larger metalla-rectangles **5**–**8** can potentially provide a site for the inclusion of small guest molecules. The *p*-cymene ruthenium analogues, [(η^6-*p*-Pr^{i}C$_6$H$_4$Me)$_4$Ru$_4$(μ-dhnq)$_2$(μ-4,4′-bipyridine)$_2$]$^{4+}$

and $[(\eta^6\text{-}p\text{-Pr}^i\text{C}_6\text{H}_4\text{Me})_4\text{Ru}_4(\mu\text{-dhnq})_2(\mu\text{-1,2-bis(4-pyridyl)ethylene})_2]^{4+}$, have been shown to encapsulate pyrene and other planar aromatic molecules in solution [36,37].

Table 1. Selected bond lengths and angles for [**3**]$(\text{CF}_3\text{SO}_3)_4$ $4\text{CH}_2\text{Cl}_2$; [**5**]$(\text{CF}_3\text{SO}_3)_4$ $2\text{CH}_2\text{Cl}_2$ and [**6**]$(\text{CF}_3\text{SO}_3)_4$ solvent.

	[**3**]$(\text{CF}_3\text{SO}_3)_4$ $4\text{CH}_2\text{Cl}_2$	[**5**]$(\text{CF}_3\text{SO}_3)_4$ $2\text{CH}_2\text{Cl}_2$	[**6**]$(\text{CF}_3\text{SO}_3)_4$ solvent
Interatomic distances (Å)			
M1-O1	2.065(3)	2.030(4)	2.073(5)
M1-O2	2.053(3)	2.028(5)	2.073(5)
M2-O3	2.061(3)	2.034(5)	2.069(5)
M2-O4	2.061(3)	2.035(4)	2.064(5)
M1-N1	2.150(3)	2.099(5)	2.116(6)
M2-N2	2.129(3)	2.094(5)	2.116(6)
M1-M2 (μ-dhnq)	8.3831(5)	8.283(1)	8.4075(6)
M1-M2 (μ-N-ligand)	6.9773(5)	11.106(1)	11.2437(7)
Angles (°)			
O1-M1-O2	87.2(1)	87.5(2)	87.4(2)
O3-M2-O4	87.4(1)	87.1(2)	87.3(2)
N1-M1-O1	84.6(1)	86.8(2)	83.1(2)
N1-M1-O2	85.7(1)	84.0(2)	83.5(2)
N2-M2-O3	84.5(1)	85.6(2)	82.9(2)
N2-M2-O4	85.7(1)	84.5(2)	84.8(2)

Figure 3. Molecular structure of metalla-rectangle **3** at 50% probability level ellipsoids with hydrogen atoms, dichloromethane molecules and triflate anions omitted for clarity.
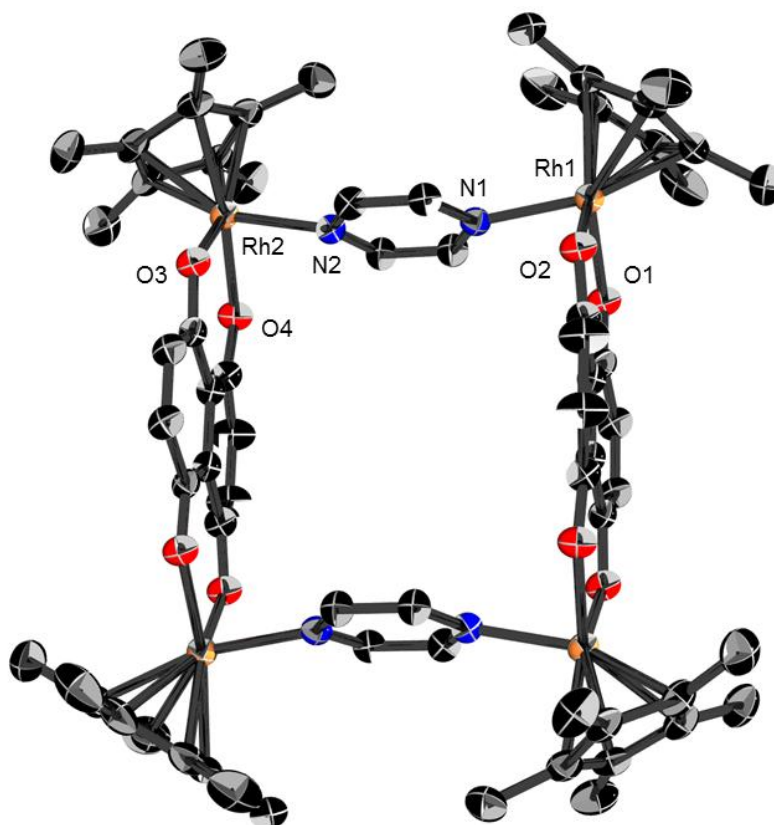
Table 2. Crystallographic and structure refinement parameters for metalla-rectangles [**3**](CF₃SO₃)₄ 4CH₂Cl₂; [**5**](CF₃SO₃)₄ 2CH₂Cl₂; and [**6**](CF₃SO₃)₄ solvent.

Parameter	[**3**](CF₃SO₃)₄ **4CH₂Cl₂**	[**5**](CF₃SO₃)₄ **2CH₂Cl₂**	[**6**](CF₃SO₃)₄ **solvent**
Chemical formula	$C_{76}H_{84}Cl_8F_{12}N_4O_{20}Rh_4S_4$	$C_{86}H_{88}Cl_4F_{12}N_4O_{20}Rh_4S_4$	$C_{84}H_{84}F_{12}Ir_4N_4O_{20}S_4$
Formula weight	2424.95	2407.28	2594.59
Crystal system	Monoclinic	Triclinic	Triclinic
Space group	*P* 2₁/*c* (no. 14)	*P*-1 (no. 2)	*P*-1 (no. 2)
Crystal color and shape	yellow block	green block	grey block
Crystal size	0.22 ×0.18 ×0.17	0.16 ×0.15 ×0.13	0.21 ×0.20 ×0.16
a (Å)	12.3640(4)	12.8157(9)	12.5846(6)
b (Å)	23.6046(6)	14.8016(10)	15.2071(7)
c (Å)	16.8800(6)	15.0871(10)	15.4594(7)
α (°)	–	90.206(5)	89.590(4)
β (°)	104.176(3)	100.106(5)	80.133(4)
γ (°)	–	106.634(5)	73.386(4)
V (Å³)	4776.4(3)	2695.2(3)	2790.4(2)
Z	2	1	1
T (K)	173(2)	173(2)	173(2)
D_c (g cm⁻³)	1.686	1.483	1.544
μ (mm⁻¹)	1.080	0.860	4.906
Scan range (°)	1.70 < θ < 29.23	1.69 < θ < 29.30	1.72 < θ < 29.22
Unique reflections	12909	14597	14976
Reflections used [I > 2σ(I)]	9875	9188	10306
R_{int}	0.0908	0.1407	0.0623
Final R indices [I > 2σ (I)]*	0.0587, *w*R₂ 0.1202	0.0881, *w*R₂ 0.2094	0.0532, *w*R₂ 0.1163
R indices (all data)	0.0836, *w*R₂ 0.1299	0.1412, *w*R₂ 0.2423	0.0915, *w*R₂ 0.1274
Goodness-of-fit	1.039	1.103	1.001
Max, Min Δρ (e Å⁻³)	1.079, −1.341	1.775, −1.254	1.925, −2.579

* Structures were refined on F_0^2: $wR_2 = [\Sigma[w (F_0^2 - F_c^2)^2]/\Sigma w (F_0^2)^2]^{1/2}$, where $w^{-1} = [\Sigma(F_0^2) + (aP)^2 + bP]$ and $P = [max(F_0^2,0) + F_c^2]/3$

As previously mentioned, in the crystal packing of **3**, **5** and **6** the solvent molecules and triflate anions are either situated at the periphery of the metalla-rectangles or positioned in the hydrophobic cavity. Despite possessing the smallest cavity, in metalla-rectangle **3** two molecules of dichloromethane sit on both sides of the metalla-cycle, see Figure 6. The shorter Cl⋯Cl separation between the two solvent molecules is 3.265(4) Å. In **5** and **6**, the cavity of the metalla-rectangles is more spacious and accordingly the guest molecules have more freedom, thus they are not as well ordered as in the crystal packing of **3**, and were not refined (see experimental part). Nevertheless, these metalla-materials can act as host compounds with appropriate guest molecules, an interesting property for biological applications [1–6].

Figure 4. Molecular structure of metalla-rectangle **5** at 50% probability level ellipsoids with hydrogen atoms, dichloromethane molecules and triflate anions omitted for clarity.
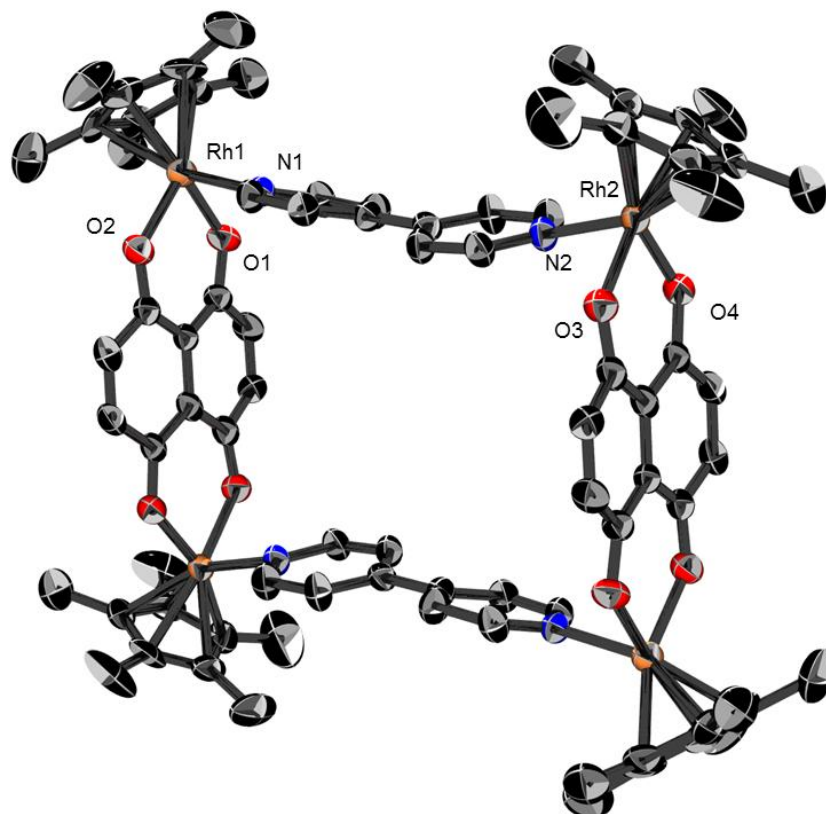

Figure 5. Molecular structure of metalla-rectangle **6** at 50% probability level ellipsoids with hydrogen atoms, solvent molecules and triflate anions omitted for clarity.
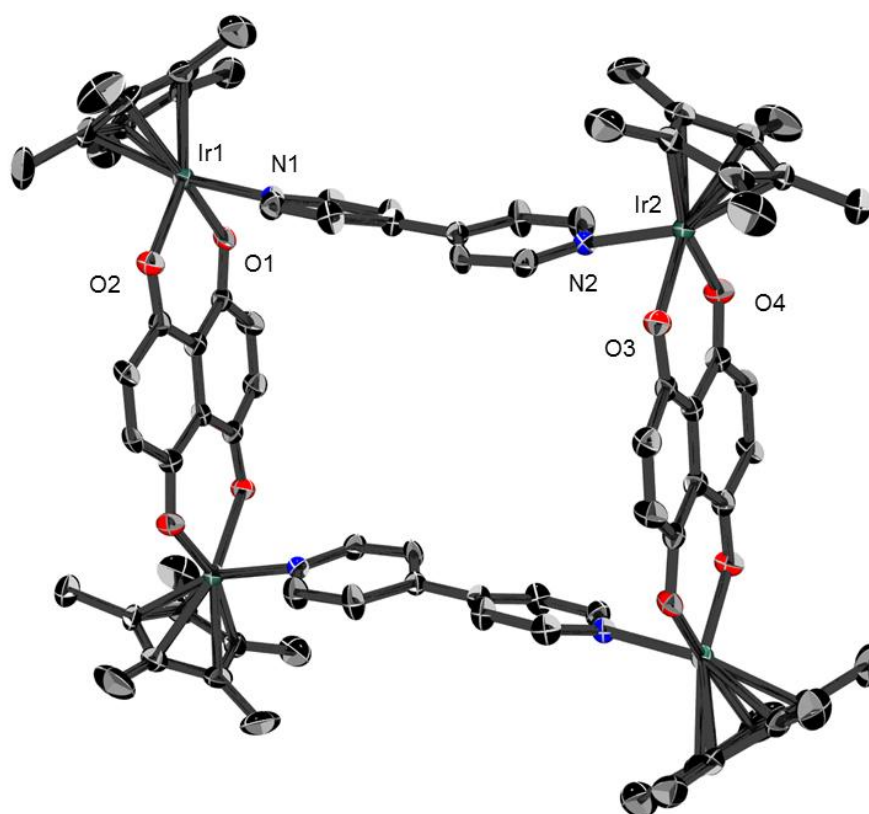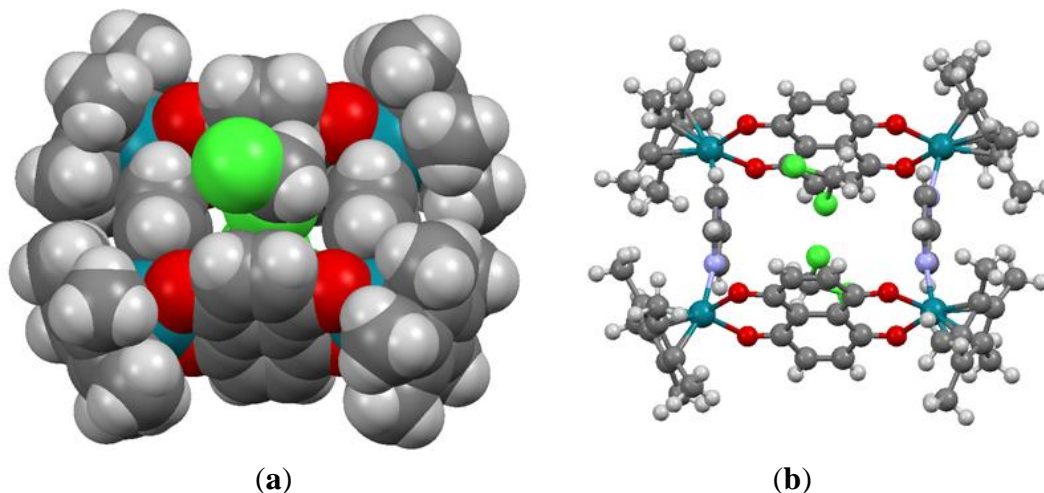
Figure 6. Space-filling (**a**) and ball-and-stick models (**b**) of metalla-rectangle **3** showing the two molecules of dichloromethane sitting on both sides of the cavity.

(**a**)   (**b**)

2.2. Antiproliferative Activity

The cytotoxicity of **3**–**8** and a Ru-analogue (Figure 1) was evaluated against human A2780 (cisplatin sensitive) and A2780cisR (cisplatin resistant) ovarian cancer cells, as well as against the non-tumorigenic HEK293 human embryonic kidney cells. The IC_{50} values after 72 h are listed in Table 3. Regarding the neutral dinuclear complexes **1** and **2**, their solubility in water was too low to allow a biological evaluation, and in DMSO the chlorido ligands were exchanged with solvent molecules.

Table 3. IC_{50} values of metalla-rectangles **3**–**8** and the Ru-analogue $[(\eta^6\text{-}p\text{-Pr}^i\text{C}_6\text{H}_4\text{Me})_4\text{Ru}_4(\mu\text{-dhnq})_2(\mu\text{-4,4}'\text{-bipyridine})_2](\text{CF}_3\text{SO}_3)_4$, toward human ovarian cancer cells A2780 and A2780cisR and healthy cells HEK293 after 72 h exposure.

	IC_{50} (μM)		
Compound	**A2780**	**A2780cisR**	**HEK293**
cisplatin	1.26 ± 0.17	19.7 ± 3.00	6.55 ± 1.00
3	0.06 ± 0.01	0.19 ± 0.01	0.17 ± 0.01
4	0.07 ± 0.01	0.25 ± 0.05	0.09 ± 0.02
5	0.08 ± 0.01	0.20 ± 0.01	0.09 ± 0.02
6	0.13 ± 0.02	0.31 ± 0.04	0.11 ± 0.02
7	0.06 ± 0.01	0.18 ± 0.01	0.10 ± 0.01
8	0.17 ± 0.01	0.29 ± 0.03	0.10 ± 0.02
Ru-analogue	1.49 ± 0.11	1.94 ± 0.07	0.77 ± 0.03

All the metalla-rectangles **3**–**8** are highly cytotoxic towards the three cell lines tested (0.06–0.31 μM), and are significantly more cytotoxic than the ruthenium analogue and cisplatin in all cases. One observable trend is that all the compounds were less active against the A2780cisR cell line compared to the A2780 cell line, indicative of a certain level of susceptibility of these compounds to the acquired cisplatin resistance mechanisms operating in the former, albeit with notably lower resistance factors (1.3–3.6) relative to cisplatin (15.6). The IC_{50} values of the compounds in the HEK293 cell line are comparable to the corresponding IC_{50} values for the A2780 cell line, with the exception of **3** which is

almost three-fold more active in the A2780 cell line (0.06 μM) compared to the HEK293 cell line (0.17 μM), indicative of a moderate level of selectivity. For compounds **3–8** the cytotoxicity appears to be independent of the choice of metal (Rh or Ir) or the ditopic nitrogen ligand present, exemplified by the similarity in IC$_{50}$ values determined for **3–8** within the three cell lines. In contrast, the activity of the Ru-analogue is significantly lower than its Rh and Ir analogues, **5** and **6**, in all three cell lines, indicating, in this case, the choice of metal (Rh and Ir *versus* Ru) is significant with respect to the level of cytotoxicity observed. Given these results it is tempting to speculate that compounds **3–8** exert their cytotoxic activity through a similar mechanism of action. Evidently on switching metal to yield the Ru-analogue the activity of the complex diminishes and is likely related to a fundamental difference in reactivity of this metalla-rectangle *in vitro*.

3. Experimental Section

3.1. General

The starting materials $[(\eta^5\text{-}C_5Me_5)Rh(\mu\text{-}Cl)Cl]_2$ and $[(\eta^5\text{-}C_5Me_5)Ir(\mu\text{-}Cl)Cl]_2$ were prepared according to published methods [38,39]. All other reagents were purchased and used without further purification. The ^{1}H and ^{13}C{^{1}H} NMR spectra were recorded with a Bruker Avance II 500 or a Bruker Avance II 400 MHz spectrometer (Bruker BioSpin GmbH, Rheinstetten, Germany) using the residual protonated solvent as an internal reference. Infrared spectra were recorded as KBr pellets with a Perkin-Elmer FTIR 1720 X spectrometer (PerkinElmer: Waltham, MA, USA). Microanalyses were carried out by the Mikroelementaranalytisches Laboratorium, ETH Zürich (Switzerland).

3.2. Synthesis of $[(\eta^5\text{-}C_5Me_5)_2Rh_2(\mu\text{-}dhnq)Cl_2]$ (**1**)

5,8-Dihydroxy-1,4-naphthoquinone (dhnqH$_2$) (30.8 mg, 0.162 mmol) was added to a solution of CH$_3$COONa (27 mg, 0.324 mmol) in methanol (30 mL). The mixture was stirred for 1 h and $[(\eta^5\text{-}C_5Me_5)_2Rh_2(\mu\text{-}Cl)_2Cl_2]$ (100 mg, 0.162 mmol) was added and stirred at room temperature. After stirring overnight the solvent was removed under reduced pressure and the solid was washed with water and dried under vacuum to give a yellow color compound. Yield 93 mg (78%). Calcd for C$_{30}$H$_{34}$Cl$_2$O$_4$Rh$_2$: C, 49.00; H, 4.66. Found: C, 48.28; H, 4.36. IR (KBr pellets, cm^{-1}): ν = 1532 s, 1418 m. ^{1}H NMR (400 MHz, CD$_2$Cl$_2$): δ = 7.01 (s, 4H, dhnq), 1.60 (s, 30H, C$_5$Me$_5$) ppm. ^{13}C{^{1}H} NMR (100 MHz, CD$_2$Cl$_2$): δ = 8.63, 92.87, 112.75, 138.66 and 171.59 ppm.

3.3. Synthesis of $[(\eta^5\text{-}C_5Me_5)_2Ir_2(\mu\text{-}dhnq)Cl_2]$ (**2**)

5,8-Dihydroxy-1,4-naphthoquinone (dhnqH$_2$) (24 mg, 0.125 mmol) was added to a solution of CH$_3$COONa (20.6 mg, 0.250 mmol) in methanol (30 mL). The mixture was stirred for 1 h and $[(\eta^5\text{-}C_5Me_5)_2Ir_2(\mu\text{-}Cl)_2Cl_2]$ (100 mg, 0.125 mmol) was added and stirred at room temperature. After stirring overnight the solvent was removed under reduced pressure and the solid was washed with water and dried under vacuum to give a grey color compound. Yield 79 mg (69%). Calcd for C$_{30}$H$_{34}$Cl$_2$O$_4$Ir$_2$: C, 39.43; H, 3.75. Found: C, 38.72; H, 3.83. IR (KBr pellets, cm^{-1}): ν = 1531 s, 1417 s. ^{1}H NMR (400 MHz, CD$_2$Cl$_2$): δ = 7.09 (s, 4H, dhnq), 1.58 (s, 30H, C$_5$Me$_5$) ppm. ^{13}C{^{1}H} NMR (100 MHz, CD$_2$Cl$_2$): δ = 8.80, 84.74, 110.39, 138.48 and 168.21 ppm.

3.4. Synthesis of [(η⁵-C₅Me₅)₄Rh₄(μ-dhnq)₂(μ-pyrazine)₂](CF₃SO₃)₄ {[3](CF₃SO₃)₄}

A mixture of **1** (60 mg, 0.081 mmol) and AgCF$_3$SO$_3$ (42 mg, 0.163 mmol) in methanol (25 mL) was stirred at room temperature for 4 h and then filtered to remove the AgCl salt formed. Pyrazine (6.5 mg, 0.081 mmol) was added to the filtrate and the solution was stirred overnight at room temperature. The solvent was removed under reduced pressure and dichloromethane (3 mL) was added. Addition of diethyl ether to the dichloromethane solution precipitated the desired product as a green powder. The powder was removed by filtration and dried under vacuum. Yield: 41 mg (49%). Calcd for [C$_{68}$H$_{76}$N$_4$O$_8$Rh$_4$] (CF$_3$SO$_3$)$_4$: C, 41.47; H, 3.67; N, 2.69. Found: C, 41.47; H, 3.88; N, 2.64. IR (KBr pellets, cm^{-1}): v = 1535 s, 1418 m, 1271 s, 1158 m, 1031 s, 639 s. ^{1}H NMR (400 MHz, CD$_2$Cl$_2$): δ = 8.81 (s, 8H, pyrazine), 7.20 (s, 8H, dhnq), 1.61 (s, 60H, C$_5$Me$_5$) ppm. ^{13}C{^{1}H} NMR (100 MHz, CD$_2$Cl$_2$): δ = 8.34, 96.30, 111.65, 139.15, 148.96 and 171.61 ppm.

3.5. Synthesis of [(η⁵-C₅Me₅)₄Ir₄(μ-dhnq)₂(μ-pyrazine)₂](CF₃SO₃)₄ {[4](CF₃SO₃)₄}

A mixture of **2** (60 mg, 0.066 mmol) and AgCF$_3$SO$_3$ (34 mg, 0.132 mmol) in methanol (25 mL) was stirred at room temperature for 4 h and then filtered to remove the AgCl salt formed. Pyrazine (5.3 mg, 0.066 mmol) was added to the filtrate and the solution was stirred overnight at room temperature. The solvent was removed under reduced pressure and dichloromethane (3 mL) was added. Addition of diethyl ether to the dichloromethane solution gave the desired product as a grey powder. The powder was removed by filtration and dried under vacuum. Yield: 43 mg (54%). Calcd for [C$_{68}$H$_{76}$N$_4$O$_8$Ir$_4$](CF$_3$SO$_3$)$_4$: C, 35.41; H, 3.14; N, 2.29. Found: C, 36.21; H, 3.48; N, 2.33. IR (KBr pellets, cm^{-1}): v = 1533 s, 1427 s, 1275 s, 1155 s, 1030 s, 637 s. ^{1}H NMR (400 MHz, CD$_2$Cl$_2$): δ = 8.88 (s, 8H, pyrazine), 7.38 (s, 8H, dhnq), 1.57 (s, 60H, C$_5$Me$_5$) ppm. ^{13}C{^{1}H} NMR (100 MHz, CD$_2$Cl$_2$): δ = 8.28, 88.51, 113.75, 139.24, 149.28 and 168.71 ppm.

3.6. Synthesis of [(η⁵-C₅Me₅)₄Rh₄(μ-dhnq)₂(μ-4,4'-bipyridine)₂](CF₃SO₃)₄ {[5](CF₃SO₃)₄}

The metalla-rectangle **5** was obtained from **1** (60 mg, 0.081 mmol), AgCF$_3$SO$_3$ (42 mg, 0.163 mmol) and 4,4′-bipyridine (12.8 mg, 0.081 mmol) following the procedure described for [**3**](CF$_3$SO$_3$)$_4$. Yield: 70 mg (77%). Calcd for [C$_{80}$H$_{84}$N$_4$O$_8$Rh$_4$](CF$_3$SO$_3$)$_4$: C, 45.09; H, 3.78; N, 2.50. Found: C, 44.77; H, 3.58; N, 2.34. IR (KBr pellets, cm^{-1}): v = 1535 s, 1414 m, 1271 s, 1157 m, 1031 s, 639 s. ^{1}H NMR (400 MHz, CD$_2$Cl$_2$): δ = 8.36 (d, 8H, ^3J = 8 Hz, bipyridine), 7.87 (d, 8H, ^3J = 8 Hz, bipyridine), 7.08 (s, 8H, dhnq), 1.47 (s, 60H, C$_5$Me$_5$) ppm. ^{13}C{^{1}H} NMR (100 MHz, CD$_2$Cl$_2$): δ = 8.42, 95.38, 111.94, 124.63, 139.16, 145.62, 151.68 and 171.58 ppm.

3.7. Synthesis of [(η⁵-C₅Me₅)₄Ir₄(μ-dhnq)₂(μ-4,4'-bipyridine)₂](CF₃SO₃)₄ {[6](CF₃SO₃)₄}

The metalla-rectangle **6** was obtained from **2** (60 mg, 0.066 mmol), AgCF$_3$SO$_3$ (34 mg, 0.132 mmol) and 4,4′-bipyridine (10.3 mg, 0.066 mmol) following the procedure described for [**4**](CF$_3$SO$_3$)$_4$. Yield: 53 mg (72%). Calcd for [C$_{80}$H$_{84}$N$_4$O$_8$Ir$_4$](CF$_3$SO$_3$)$_4$ 6 H$_2$O: C, 37.33; H, 3.58; N, 2.07. Found: C, 36.79; H, 3.58; N, 2.82. IR (KBr pellets, cm^{-1}): v = 1533 s, 1427 m, 1276 s, 1156 m, 1031 s, 639 s. ^{1}H NMR (400 MHz, CD$_2$Cl$_2$): δ = 8.47 (d, 8H, ^3J = 8 Hz, bipyridine), 8.05 (d, 8H, ^3J = 8 Hz,

bipyridine), 7.31 (s, 8H, dhnq), 1.54 (s, 60H, C$_5$Me$_5$) ppm. ^{13}C{^{1}H} NMR (100 MHz, CD$_2$Cl$_2$): δ = 8.45, 87.41, 13.92, 124.99, 139.18, 145.18, 151.34 and 168.54 ppm.

3.8. Synthesis of [(η^5-C$_5$Me$_5$)$_4$Rh$_4$(μ-dhnq)$_2$(μ-1,2-bis(4-pyridyl)ethane)$_2$](CF$_3$SO$_3$)$_4$ {[7](CF$_3$SO$_3$)$_4$}

The metalla-rectangle **7** was obtained from **1** (60 mg, 0.081 mmol), AgCF$_3$SO$_3$ (42 mg, 0.163 mmol) and 1,2-bis(4-pyridyl)ethylene (14.9 mg, 0.081 mmol) following the procedure described for [**3**](CF$_3$SO$_3$)$_4$. Yield: 75 mg (81%). Calcd for [C$_{84}$H$_{88}$N$_4$O$_8$Rh$_4$](CF$_3$SO$_3$)$_4$: C, 46.16; H, 3.87; N, 2.45. Found: C, 45.66; H, 3.53; N, 2.45. IR (KBr pellets, cm^{-1}): ν = 1535 s, 1417 m, 1271 s, 1160 m, 1032 s, 639 s. ^{1}H NMR (400 MHz, CD$_2$Cl$_2$): δ = 8.27 (d, 8H, ^3J = 8 Hz, pyridyl), 7.70 (d, 8H, ^3J = 8 Hz, pyridyl), 7.42 (s, 4H, CH=CH), 7.16 (s, 8H, dhnq), 1.57 (s, 60H, C$_5$Me$_5$) ppm. ^{13}C{^{1}H} NMR (100 MHz, CD$_2$Cl$_2$): δ = 8.44, 95.26, 111.86, 124.93, 131.77, 139.10, 146.68, 150.71 and 171.50 ppm.

3.9. Synthesis of [(η^5-C$_5$Me$_5$)$_4$Ir$_4$(μ-dhnq)$_2$(μ-1,2-bis(4-pyridyl)ethane)$_2$](CF$_3$SO$_3$)$_4$ {[8](CF$_3$SO$_3$)$_4$}

The metalla-rectangle **8** was obtained from **2** (60 mg, 0.066 mmol), AgCF$_3$SO$_3$ (34 mg, 0.132 mmol) and 1,2-bis(4-pyridyl)ethylene (12 mg, 0.066 mmol) following the procedure described for [**4**](CF$_3$SO$_3$)$_4$. Yield: 60 mg (69%). Calcd for [C$_{84}$H$_{88}$N$_4$O$_8$Ir$_4$](CF$_3$SO$_3$)$_4$ 6 H$_2$O: C, 38.37; H, 3.66; N, 2.03. Found: C, 38.02; H, 3.58; N, 2.12. IR (KBr pellets, cm^{-1}): ν = 1532 s, 1427 m, 1275 s, 1157 m, 1031 s, 639 s. ^{1}H NMR (400 MHz, CD$_2$Cl$_2$): δ = 8.28 (d, 8H, ^3J = 8 Hz, pyridyl), 7.78 (d, 8H, ^3J = 8 Hz, pyridyl), 7.49 (s, 4H, CH=CH), 7.29 (s, 8H, dhnq), 1.53 (s, 60H, C$_5$Me$_5$) ppm. ^{13}C{^{1}H} NMR (100 MHz, CD$_2$Cl$_2$): δ = 8.48, 87.19, 113.86, 125.30, 131.89, 139.10, 147.08, 150.26 and 168.41 ppm.

3.10. Cell Culture and Inhibition of Cell Growth

Human A2780 and A2780cisR ovarian carcinoma cells and HEK293 cells were obtained from the European Collection of Cell Cultures (ECACC) (Salisbury, UK). Cells were cultured in either RPMI-1640 with GlutaMAX (A2780, A2780cisR) or DMEM (Dulbecco's Modified Eagle Medium) high glucose with GlutaMAX (HEK 293) medium containing 10% fetal bovine serum (FBS) and penicillin at 37 °C and 5% CO$_2$. Cytotoxicity was determined using the MTT (3-(4,5-dimethylthiazol-2-yl)-2,5-diphenyltetrazolium bromide) assay (see below). Cells were seeded in 96 well plates by the addition of cells as a suspension in their respective media containing 10% FBS (100 μL per well, approximately 4300 cells) and pre-incubated for 24 h.

Fresh stock solutions of the compounds were prepared in DMSO just before injections, then the stock solution were diluted by addition to the culture medium [RPMI (Roswell Park Memorial Institute medium) or DMEM for A2780 and A2780cisR or HEK 293, respectively]. The stock solutions were serially diluted to give compound solutions of the desired concentrations. Complex solutions (100 μL) were then added to plate wells (yielding final compound solutions in the range 0 to 5 μM) and the plates incubated for a further 72 h.

Subsequently, MTT (3-(4,5-dimethyl-2-thiazolyl)-2,5-diphenyl-2H-tetrazolium bromide) solution (20 μL, 5 mg/mL in H$_2$O) was added to each well and the plates incubated for a further 2 h. The culture medium was then aspirated and the violet formazan precipitate produced by mitochondrial dehydrogenases of living cells was dissolved by the addition of DMSO (100 μL) to each well. The

absorbance of the resultant solutions at 590 nm, which is directly proportional to the number of surviving cells, was recorded using a multiwell plate reader. The percentage of surviving cells was determined by measurement of the absorbance of wells corresponding to untreated control cells. The reported IC_{50} values are based on the mean values from two independent experiments; each concentration level per experiment was evaluated in triplicate, and those values are reported in Table 3.

3.11. Single-Crystal X-ray Structure Analysis

Crystals of compounds [**3**](CF_3SO_3)$_4$, [**5**](CF_3SO_3)$_4$ and [**6**](CF_3SO_3)$_4$ were mounted on a Stoe Image Plate Diffraction system equipped with a ϕ circle goniometer, using Mo-Kα graphite monochromatic radiation ($\lambda = 0.71073$ Å) with ϕ range 0–200 °. The structures were solved by direct methods using the program SHELXS-97, while the refinement and all further calculations were carried out using SHELXL-97 [40]. The H-atoms were included in calculated positions and treated as riding atoms using the SHELXL default parameters. The non-H atoms were refined anisotropically, using weighted full-matrix least-square on F^2. In **6**, the solvent molecules were highly disordered and a data set corresponding to omission of the missing solvent was generated using the SQUEEZE algorithm [41] and the structure was refined to convergence. These missing solvent molecules are probably dichloromethane molecules, which fit perfectly with the size of the voids, the electron counts and the crystal packing of compound [**5**](CF_3SO_3)$_4$, which possesses two molecules of dichloromethane per asymmetric unit. Crystallographic details for [**3**](CF_3SO_3)$_4$, [**5**](CF_3SO_3)$_4$ and [**6**](CF_3SO_3)$_4$ are summarized in Table 2. Figures 3, 4 and 5 were drawn with ORTEP [42] and Figure 6 was drawn with Mercury [43].

CCDC-959397 [**3**](CF_3SO_3)$_4$ 4CH_2Cl_2, 959398 [**5**](CF_3SO_3)$_4$ 2CH_2Cl_2 and 959399 [**6**](CF_3SO_3)$_4$ solvent contain the supplementary crystallographic data for this paper. These data can be obtained free of charge at www.ccdc.cam.ac.uk/conts/retrieving.html [or from the Cambridge Crystallographic Data Centre, 12, Union Road, Cambridge CB2 1EZ, UK; fax: (internat.) +44-1223/336-033; E-mail: deposit@ccdc.cam.ac.uk].

4. Conclusions

The antiproliferative activities of a series of half-sandwich Rh(III) and Ir(III) tetranuclear metalla-cycles have been evaluated *in vitro* against the human ovarian A2780 (cisplatin sensitive) and A2780cisR (cisplatin resistant) cancer cell lines and on non-tumorigenic human embryonic kidney HEK293 cells. These metalla-rectangles have been found to be highly cytotoxic with IC_{50} in the low micromolar range. The cationic charge, the size, the nature of the metal ion, and the presence of a hydrophobic cavity in these metalla-materials, are all plausible factors which can contribute to their high biological activity. These results further confirm the great potential of metalla-materials in the field of biology [1−6].

Acknowledgments

Conflicts of Interest

The authors declare no conflict of interest.

References

1. Cook, T.R.; Vajpayee, V.; Lee, M.H.; Stang, P.J.; Chi, K.-W. Biomedical and biochemical applications of self-assembled metallacycles and metallacages. *Acc. Chem. Res.* **2013**, *46*, 2464–2474.
2. Therrien, B. Drug delivery by water-soluble organometallic cages. *Top Curr. Chem.* **2012**, *319*, 35–56.
3. Smith, G.S.; Therrien, B. Targeted and multifunctional arene ruthenium chemotherapeutics. *Dalton Trans.* **2011**, *40*, 10793–10800.
4. Mishra, A.; Kang, S.C.; Chi, K.-W. Coordination-driven self-assembly of arene-ruthenium compounds. *Eur. J. Inorg. Chem.* **2013**, 5222–5232.
5. Hartinger, C.G.; Phillips, A.D.; Nazarov, A.A. Polynuclear ruthenium, osmium and gold complexes. The quest for innovative chemotherapeutics. *Curr. Top Med. Chem.* **2011**, *11*, 2688–2702.
6. Hartinger, C.G.; Metzler-Nolte, N.; Dyson, P.J. Challenges and opportunities in the development of organometallic anticancer drugs. *Organometallics* **2012**, *31*, 5677–5685.
7. Mattsson, J.; Govindaswamy, P.; Renfrew, A.K.; Dyson, P.J.; Štěpnička, P.; Süss-Fink, G.; Therrien, B. Synthesis, molecular structure, and anticancer activity of cationic arene ruthenium metallarectangles. *Organometallics* **2009**, *28*, 4350–4357.
8. Barry, N.P.E.; Zava, O.; Furrer, J.; Dyson, P.J.; Therrien, B. Anticancer activity of opened arene ruthenium metalla-assemblies. *Dalton Trans.* **2010**, *39*, 5272–5277.
9. Barry, N.P.E.; Edafe, F.; Therrien, B. Anticancer activity of tetracationic arene ruthenium metalla-cycles. *Dalton Trans.* **2011**, *40*, 7172–7180.
10. Vajpayee, V.; Song, Y.H.; Yang, Y.J.; Kang, S.C.; Cook, T.R.; Kim, D.W.; Lah, M.S.; Kim, I.S.; Wang, M.; Stang, P.J.; *et al.* Self-assembly of cationic, hetero- or homonuclear ruthenium(II) macrocyclic rectangles and their photophysical, electrochemical, and biological studies. *Organometallics* **2011**, *30*, 6482–6489.
11. Vajpayee, V.; Lee, S.m.; Park, J.W.; Dubey, A.; Kim, H.; Cook, T.R.; Stang, P.J.; Chi, K.-W. Growth inhibitory activity of a bis-benzimidazole-bridged arene ruthenium metalla-rectangle and -prism. *Organometallics* **2013**, *32*, 1563–1566.
12. Jung, H.; Dubey, A.; Koo, H.J.; Vajpayee, V.; Cook, T.R.; Kim, H.; Kang, S.C.; Stang, P.J.; Chi, K.-W. Self-assembly of ambidentate pyridyl-carboxylate ligands with octahedral ruthenium metal centers: Self-selection for a single-linkage isomer and anticancer-potency studies. *Chem. Eur. J.* **2013**, *19*, 6709–6717.
13. Linares, F.; Galindo, M.A.; Galli, S.; Romero, M.A.; Navarro, J.A.R.; Barea, E. Tetranuclear coordination assemblies based on half-sandwich ruthenium(II) complexes: Noncovalent binding to DNA and cytotoxicity. *Inorg. Chem.* **2009**, *48*, 7413–7420.

14. Linares, F.; Procopio, E.Q.; Galindo, M.A.; Romero, M.A.; Navarro, J.A.R.; Barea, E. Molecular architecture of redox-active half-sandwich Ru(II) cyclic assemblies. Interactions with biomolecules and anticancer activity. *CrystEngComm* **2010**, *12*, 2343–2346.

15. Vajpayee, V.; Song, Y.H.; Lee, M.H.; Kim, H.; Wang, M.; Stang, P.J.; Chi, K.-W. Self-assembled arene-ruthenium-based rectangles for the selective sensing of multi-carboxylate anions. *Chem. Eur. J.* **2011**, *17*, 7837–7844.

16. Severin, K. Research in the laboratory of supramolecular chemistry: Functional nanostructures, sensors, and catalysts. *Chimia* **2011**, *65*, 680–682.

17. Gao, J.; Rochat, S.; Qian, X.; Severin, K. A simple assay for the fluorometric detection of lithium ions in aqueous solution. *Chem. Eur. J.* **2010**, *16*, 5013–5017.

18. Mendoza-Ferri, M.-G.; Hartinger, C.G.; Eichinger, R.E.; Stolyarova, N.; Severin, K.; Jakupec, M.A.; Nazarov, A.A.; Keppler, B.K. Influence of the spacer length on the *in vitro* anticancer activity of dinuclear ruthenium-arene compounds. *Organometallics* **2008**, *27*, 2405–2407.

19. Mendoza-Ferri, M.-G.; Hartinger, C.G.; Nazarov, A.A.; Kandioller, W.; Severin, K.; Keppler, B.K. Modifying the structure of dinuclear ruthenium complexes with antitumor activity. *Appl. Organometal. Chem.* **2008**, *22*, 326–332.

20. Liu, H.-K.; Sadler, P.J. Metal complexes as DNA intercalators. *Acc. Chem. Res.* **2011**, *44*, 349–359.

21. Barry, N.P.E.; Edafe, F.; Dyson, P.J.; Therrien, B. Anticancer activity of osmium metalla-rectangles. *Dalton Trans.* **2010**, *39*, 2816–2820.

22. Severin, K.; Bergs, R.; Beck, W. Bioorganometallic chemistry-transition metal complexes with α-amino acids and peptides. *Angew. Chem. Int. Ed.* **1998**, *37*, 1634–1654.

23. Herberhold, M.; Yan, H.; Milius, W.; Wrackmeyer, B. Metal-induced B-H activation: Addition of methyl acetylene carboxylates to Cp*Rh-, Cp*Ir-, (*p*-cymene)Ru-, and (*p*-cymene)Os half-sandwich complexes containing the chelating 1,2-dicarba-*closo*-dodecaborane-1,2-dithiolate ligand. *Chem. Eur. J.* **2000**, *6*, 3026–2032.

24. Hartinger, C.G.; Dyson, P.J. Bioorganometallic chemistry—From teaching paradigms to medicinal applications. *Chem. Soc. Rev.* **2009**, *38*, 391–401.

25. Gupta, G.; Garci, A.; Murray, B.S.; Dyson, P.J.; Fabre, G.; Trouillas, P.; Giannini, F.; Furrer, J.; Süss-Fink, G.; Therrien, B. Synthesis, molecular structure, computational study and *in vitro* anticancer activity of dinuclear thiolato-bridged pentamethylcyclopentadienyl Rh(II) and Ir(II) complexes. *Dalton Trans.* **2013**, *42*, 15457–15463.

26. Dorcier, A.; Ang, W.H.; Bolaño, S.; Gonsalvi, L.; Juillerat-Jeanneret, L.; Laurenczy, G.; Peruzzini, M.; Phillips, A.D.; Zanobini, F.; Dyson, P.J. *In vitro* evaluation of rhodium and osmium RAPTA analogues: The case for organometallic anticancer drugs not based on ruthenium. *Organometallics* **2006**, *25*, 4090–4096.

27. Hearn, J.M.; Romero-Canelón, I; Qamar, B.; Liu, Z.; Hands-Portman, I.; Sadler, P.J. Organometallic iridium(III) anticancer complexes with new mechanisms of action: NCI-60 screening mitochondrial targeting, and apoptosis. *ACS Chem. Biol.* **2013**, *8*, 1335–1343.

28. Barry, N.P.E.; Sadler, P.J. Exploration of the medical periodic table: Towards new targets. *Chem. Commun.* **2013**, *49*, 5106–5131.

29. Geldmacher, Y.; Oleszak, M.; Sheldrick, W.S. Rhodium(III) and iridium(III) complexes as anticancer agents. *Inorg. Chim. Acta* **2012**, *393*, 84–102.

30. Han, Y.-F.; Jia, W.-G.; Yu, W.-B.; Jin, G.-X. Stepwise formation of organometallic macrocycles, prisms and boxes from Ir, Rh and Ru-based half-sandwich units. *Chem. Soc. Rev.* **2009**, *38*, 3419–3434.

31. Han, Y.-F.; Lin, Y.-J.; Jin, G.-X. Discrete half-sandwich Ir, Rh-based organometallic molecular boxes: Synthesis, characterization, and their properties. *Dalton Trans.* **2011**, *40*, 10370–10375.

32. Wu, T.; Lin, Y.-J.; Jin, G.-X. Stepwise formation of organometallic macrocycles and triangular prisms containing 2,2'-bisbenzimidazole ligands. *Dalton Trans.* **2013**, *42*, 82–88.

33. Yan, H.; Süss-Fink, G.; Neels, A.; Stoeckli-Evans, H. Mono-, di- and tetra-nuclear *p*-cymeneruthenium complexes containing oxalato ligands. *J. Chem. Soc. Dalton Trans.* **1997**, 4345–4350.

34. Pitto-Barry, A.; Barry, N.P.E.; Zava, O.; Deschenaux, R.; Therrien, B. Encapsulation of pyrene-functionalized poly(benzyl ether) dendrons into a water-soluble organometallic cages. *Chem. Asian J.* **2011**, *6*, 1595–1603.

35. Huang, S.-L.; Lin, Y.-J.; Hor, T.S.A.; Jin, G.-X. Cp*Rh-based heterometallic metallarectangles: Size-dependent borromean link structures and catalytic acyl transfer. *J. Am. Chem. Soc.* **2013**, *135*, 8125–8128.

36. Barry, N.P.E.; Furrer, J.; Therrien, B. In- and out-of-cavity interactions by modulating the size of ruthenium metallarectangles. *Helv. Chim. Acta* **2010**, *93*, 1313–1328.

37. Barry, N.P.E.; Furrer, J.; Freudenreich, J.; Süss-Fink, G.; Therrien, B. Designing the host-guest properties of tetranuclear arene ruthenium metalla-rectangles to accommodate a pyrene molecule. *Eur. J. Inorg. Chem.* **2010**, 725–728.

38. Kang, J.W.; Moseley, K.; Maitlis, P.M. Pentamethylcyclopentadienylrhodium and -iridium halides. Synthesis and properties. *J. Am. Chem. Soc.* **1969**, *91*, 5970–5977.

39. White, C.; Yates, A.; Maitlis, P.M.; Heinekey, D.M. (η^5-Pentamethylcyclopenta-dienyl)rhodium and -iridium compounds. *Inorg. Synth.* **1992**, *29*, 228–234.

40. Sheldrick, G.M. A short history of SHELX. *Acta Cryst.* **2008**, *64*, 112–122.

41. Spek, A.L. Single-crystal structure validation with the program PLATON. *J. Appl. Cryst.* **2003**, *36*, 7–13.

42. Farrugia, L.J. ORTEP-3 for Windows—A version of ORTEP-III with a graphical interface (GUI) *J. Appl. Cryst.* **1997**, *30*, 565.

43. Bruno, I.J.; Cole, J.C.; Edington, P.R.; Kessler, M.; Macrae, C.F.; McCabe, P.; Pearson, J.; Taylor, R. New software for searching the Cambridge Structural Database and visualizing crystal structures. *Acta Cryst.* **2002**, *58*, 389–397.